Cramer-Rao bounds for Channel Estimation in UWB Impulse Radio

Philippe Ciblat$^{(*)}$, Anne-Laure Deleuze and Christophe J. Le Martret

Abstract

This paper addresses the Cramer-Rao bound calculation for channel parameter estimation in impulse radio ultra-wide band systems. We consider a time-hopping code scheme with binary pulse position and pulse amplitude modulation formats. We first derive in closed-form the (resp. modified) Cramer-Rao bound for the multipath channel parameters in the data-aided (resp. non-data-aided) context. Unlike existing methods, the calculations are derived taking into account the overlapping between signal echoes due to multipaths. We illustrate the benefit of taking into account the overlapping assumption on realistic channel propagation environment. Simulations show that the Cramer-Rao bound using the non-overlapping assumption clearly overestimate the performance.

$^{(*)}$ Corresponding author.

Christophe Le Martret is with THALES Land and Joint Systems, Colombes, France (`christophe.le_martret@fr.thalesgroup.com`). Philippe Ciblat and Anne-Laure Deleuze are with Ecole Nationale Supérieure des Télécommunications (ENST), Département Communications et Electronique, Paris, France (`philippe.ciblat@enst.fr,deleuze@enst.fr`).

This paper has been partially published in IEEE Workshop on Signal Processing Advances in Wireless Communications (SPAWC), Lisbon (Portugal), July 2004.

I. INTRODUCTION

For the last decade, impulse radio ultra-wide band (IR-UWB) communication systems have received increasing interest, for both personal area networks (short range, high data rate) and sensor networks (long/medium range, low data rate). A lot of work has been done on the receiver design and the multiple-access performance analysis [1], [2], assuming perfect knowledge of the propagation channel at the receiver side. Several papers focus on channel estimator design based on maximum-likelihood (ML) [3], [4] or bases on ad hoc methods [5], [6].

In the literature, only a few papers address the evaluation of the Cramer-Rao bound (CRB) in closed-form [7], [8], [9], [10]. CRB derivations for the channel parameters in the context of TH-IR-UWB have been addressed in the data-aided (DA) context [7], [8], [9] and in the non-data-aided (NDA) context [10]. In [7], a single path channel is considered, and in the other papers, the computations are derived assuming that the pulses of the multipaths do not overlap. In [10], the so-called *true* CRB in the NDA context is expressed in closed-form, assuming non-overlapping pulses and other restrictive assumptions on the channel delays. In [9], the authors acknowledge that the non-overlapping assumption does not hold all the time. They show that the CRB calculated without the non-overlapping assumption is always greater than the CRB evaluated under the overlapping one, without providing closed-form expressions for the later case though.

Therefore, the purpose of this paper is to derive in closed-form the CRB of the channel parameter estimation (attenuations and delays) under the overlapping assumption for TH-IR-UWB systems using PAM and PPM formats. The derivations are done both in the DA and NDA contexts. Notice that in the NDA context, we address the so-called *Modified* CRB (MCRB) [11].

The paper is organized as follows: in Section II, we present the signal model, the CRB definition as well as some preliminary derivations. Section III introduces the main contribution of this paper since the Fisher information matrix is derived in closed-form whether the paths overlap or not. In section IV, we compare the numerical values of both CRBs in order to observe the influence of the overlapping path assumption on the performance. We also compare the CRB with the performance of some existing estimation algorithms. Concluding remarks and perspectives are drawn in Section V.

II. System Model and Preliminaries

We consider that the received signal $y(t)$ takes the following form

$$y(t) = \sum_{l=1}^{L} A_l s(t - \tau_l) + w(t)$$

where $s(t)$ represents the UWB signal waveform of the user of interest. The noise $w(t)$ is assumed to be white and Gaussian with variance $\sigma^2 = \mathbb{E}[w(t)^2] = N_0/2$. The noise represents the thermal noise in the single carrier case and can also approximate the multiple access interference in the multiuser case when conditions are met [12], [13]. The propagation channel response is modeled with Dirac functions as done in recent papers [14], [4]. The parameters A_l and τ_l correspond to the attenuation and the delay of the l^{th} path respectively and need to be estimated. The attenuations and the delays are stacked in $\mathbf{A} = [A_1, \cdots, A_L]$ and $\boldsymbol{\tau} = [\tau_1, \cdots, \tau_L]$ respectively. In previous works, authors usually assume that the maximum delay τ_L is less than a symbol duration in order to simplify the computation [2], [4], [10]. However, this assumption does not hold in high data rate scenario and in dense multipath channels with long delay spread. Consequently, in the following we will consider no constraint on the maximum delay and inter-symbol interference may occur.

.0.a PPM format. The UWB waveform using binary PPM can be defined as follows

$$s(t) = \sum_{i=0}^{M-1} b(t - iN_f T_f - d_i \Delta) \tag{1}$$

where M is the number of transmit symbols $d_i \in \{0, 1\}$. We define $\mathbf{d} = [d_0, \cdots, d_{M-1}]$. In the DA context, $\mathbf{d}$ is known at the receiver and thus is referred to as the training sequence. In NDA context, the symbols are assumed to be unknown, independent and identically distributed (i.i.d.), and equally likely distributed, *i.e.* $\Pr\{d_i = 0\} = \Pr\{d_i = 1\} = 0.5$. The variable Δ represents the PPM delay shift, N_f is the number of frame per symbol and T_f is the frame duration. The super frame, composed of N_f frames is structured as follows:

$$b(t) = \sum_{j=0}^{N_f-1} g(t - jT_f - \tilde{c}_j T_c) \tag{2}$$

where T_c is the chip duration, $T_f = N_c T_c$ with N_c the number of chips per frame, $\tilde{c}_j \in \{0, \cdots, N_c - 1\}$ the time-hopping code of the j^{th} frame, and $g(t)$ is the received pulse[1] with time duration $[0, T_g)$ where $T_g < T_c$. Notice that we use the conventional assumption, $0 < \Delta < T_c - T_g$, *i.e.*, the pulse duration associated with the transmit bit (whatever its value) remains inside the current chip duration.

.0.b PAM format. For the PAM format, the transmit signal takes the following form

$$s(t) = \sum_{i=0}^{M-1} d_i b(t - iN_f T_f) \tag{3}$$

where $d_i \in \{-1, +1\}$ are the PAM symbols. In the NDA context, the symbols are assumed to be unknown, i.i.d., and equally likely distributed.

In the sequel, we firstly consider the DA case. We will see later that the NDA case can be treated similarly. In order to derive the CRB, we now introduce the likelihood function of the parameter of interest $\mathbf{A}$, $\boldsymbol{\tau}$, and the corresponding Fisher information matrix (FIM). Since $\mathbf{d}$ is deterministic (DA context), the likelihood is thus given by:

$$\Lambda_{\mathbf{d}}(\mathbf{A}, \boldsymbol{\tau}) \propto \exp\left\{ -\frac{1}{N_0} \int_{\mathcal{I}} \left[y(t) - \sum_{l=0}^{L} A_l s(t - \tau_l) \right]^2 dt \right\} \tag{4}$$

where $\mathcal{I} = [0, MN_f T_f)$ represents the observation duration window.

We now define the Fisher information component for parameters (θ_l, θ_k) as follows

$$J(\theta_l, \theta_k) = -\mathbb{E}_y \left[\frac{\partial^2 \ln \Lambda_{\mathbf{d}}(\mathbf{A}, \boldsymbol{\tau})}{\partial \theta_l \partial \theta_k} \right] \tag{5}$$

with $\boldsymbol{\theta} = [\mathbf{A}, \boldsymbol{\tau}]$. Replacing (4) back in (5) leads to the following result after straightforward algebraic manipulations:

$$\begin{aligned} J(A_l, A_k) &= \frac{2}{N_0} f_1^{(k,l)} \\ J(A_l, \tau_k) &= -\frac{2A_k}{N_0} f_2^{(l,k)} \\ J(\tau_l, \tau_k) &= \frac{2A_k A_l}{N_0} f_3^{(k,l)} \end{aligned}$$

[1]this pulse encompasses the transmit pulse, the transmit front-end, and the receive front-end and is assumed to be known at the receiver side

where

$$
\begin{aligned}
f_1^{(k,l)} &= \int_{\mathcal{I}} s(t-\tau_k)s(t-\tau_l)dt \\
f_2^{(k,l)} &= \int_{\mathcal{I}} s(t-\tau_k)s'(t-\tau_l)dt \\
f_3^{(k,l)} &= \int_{\mathcal{I}} s'(t-\tau_k)s'(t-\tau_l)dt
\end{aligned}
$$

with $s'(t)$ the first derivative function of $t \mapsto s(t)$.

One can notice that the previous expressions have been obtained without any particular assumption on the transmit signal $s(t)$. In the previous works [7], [8], [10], the authors consider that $f_m^{(k,l)} = 0$ when $k \neq l$, which is equivalent to make the non-overlapping assumption. In that case, the FIM turns out to be a diagonal matrix and only the terms $f_m^{(k,l)}$ for $k = l$ need to be evaluated which makes the CRB derivations much easier than when assuming non-overlapping assumption.

In the next section, we derive closed-form expressions for $f_m^{(k,l)}$ $\forall\, k, l$ by replacing $s(t)$ with its UWB expression and considering the overlapping assumption.

III. Cramer-Rao Bound derivations

In this section we expose in details the CRB derivation for the PPM format. Results for the PAM format can be obtained similarly and will be given at the end of the section.

The derivation of $f_m^{(k,l)}$ expressions is facilitated thanks to the so-called *developed code* introduced in [16]. The developed code is a nice tool and a relevant way for describing the time-hopping code by putting the code contribution outside the argument of the pulse, thus allowing to derive simple closed-form expressions. Let us now recall the notion of developed code. The integer $\tilde{c}_j$ represents the chip number in which the signal has been put in the j^{th} frame, and belongs to the set $\{0, \cdots, N_c - 1\}$. As in [16], we now consider the vector $\mathbf{c}_j = [c_j(0), \cdots, c_j(N_c - 1)]$ of size $1 \times N_c$ described as follows:

$$
c_j(i) = \begin{cases} 1 & \text{if } i = \tilde{c}_j \\ 0 & \text{otherwise} \end{cases} .
$$

Both $\tilde{c}_j$ and the developed code $\mathbf{c}_j$ contain the same information. Instead of providing the number of the occupied chip, the developed code indicates whether the pulse belongs to the chip (if the value is equal to 1) or not (if the value is equal to 0). Finally, we concatenate all the vectors $\mathbf{c}_j$ into the following $1 \times N_f N_c$ vector $\mathbf{c} = [\mathbf{c}_0, \cdots, \mathbf{c}_{N_f-1}]$. The entries of $\mathbf{c}$ are defined as follows $\{c(j)\}_{0 \leq j < N_f N_c}$. According to the developed code, $b(t)$ takes now the following form

$$b(t) = \sum_{j=0}^{N_f N_c - 1} c(j) g(t - jT_c).$$

Before going further, we need to decompose the path difference as follows

$$\tau_k - \tau_l = Q_{k,l} N_f T_f + q_{k,l} T_c + \varepsilon_{k,l} \tag{6}$$

with $Q_{k,l} = \mathrm{int}[(\tau_k - \tau_l)/N_f T_f]$ and $q_{k,l} = \mathrm{int}[(\tau_k - \tau_l - Q_{k,l} N_f T_f)/T_c]$, where $\mathrm{int}[x]$ is the floor integer part of x defined by $\mathrm{int}[x] \leq x < \mathrm{int}[x] + 1$, and where $\varepsilon_{k,l}$ represents the remainder. By definition, we have $q_{k,l} \in \{0, \cdots, N_c N_f - 1\}$, and $\varepsilon_{k,l} \in [0, T_c)$. Moreover, the terms $Q_{k,l}$, $q_{k,l}$, and $\varepsilon_{k,l}$ depend on $(\tau_k - \tau_l)$ even if this dependency is not mentioned in the sequel. Moreover we can reasonnably assume that $Q_{k,l} \in \{-M, M-1\}$, that is to say that, the maximum delay is smaller than the observation window duration. Unlike usually done [2], [4], [10], we do not constraint the maximum delay to be less than the symbol duration.

The decomposition (6) enables us to treat the problem of the overlapping case more easily. The path difference is split into three terms describing different order of granularity: the first one deals with the overlapping due to the shift between symbols (given by $Q_{k,l}$); the second one deals with the overlapping due to the shift between chips (given by $q_{k,l}$); and the third one deals with the position inside the considered chips (given by $\varepsilon_{k,l}$).

In Appendix, we establish the following property which provides a closed-form expression for the FIM in the DA context.

*Property 1: If a **PPM** format is used and since the time support of $s \to r_m(s)$ is smaller than T_c and $\Delta < T_c - T_g$, we get*

$$\begin{aligned} f_m^{(k,l)} &= M\big[\mathcal{C}^-(q_{k,l})\mathcal{A}_m(\varepsilon_{k,l}) \\ &+ \mathcal{C}^-(q_{k,l}+1)\mathcal{A}_m(\varepsilon_{k,l} - T_c) \\ &+ \mathcal{C}^+(q_{k,l})\mathcal{B}_m(\varepsilon_{k,l}) \\ &+ \mathcal{C}^+(q_{k,l}+1)\mathcal{B}_m(\varepsilon_{k,l} - T_c)\big] \end{aligned} \tag{7}$$

with

$$\mathcal{C}^-(q) = \sum_{k=0}^{q-1} c(k)c(k-q). \tag{8}$$

$$\mathcal{C}^+(q) = \sum_{k=q}^{N_cN_f-1} c(k)c(k-q). \tag{9}$$

and with

$$\mathcal{A}_m(\varepsilon_{k,l}) = \frac{1}{M}\sum_{i=0}^{M-1} r_m(\varepsilon_{k,l} + \Delta(d_{i-Q_{k,l}-1} - d_i))$$

$$\mathcal{B}_m(\varepsilon_{k,l}) = \frac{1}{M}\sum_{i=0}^{M-1} r_m(\varepsilon_{k,l} + \Delta(d_{i-Q_{k,l}} - d_i))$$

where $Q_{k,l}$, $q_{k,l}$, and $\varepsilon_{k,l}$ are defined in (6).

The FIM calculation in closed-form for the PAM format can be done in a similar way and is summarized in the following property.

*Property 2: If a **PAM** format is used and since the time support of $s \to r_m(s)$ is smaller than T_c, we get*

$$\begin{aligned} f_m^{(k,l)} &= M\big[\mathcal{C}^-(q_{k,l})\tilde{\mathcal{A}}_m(\varepsilon_{k,l}) \\ &+ \mathcal{C}^-(q_{k,l}+1)\tilde{\mathcal{A}}_m(\varepsilon_{k,l} - T_c) \\ &+ \mathcal{C}^+(q_{k,l})\tilde{\mathcal{B}}_m(\varepsilon_{k,l}) \\ &+ \mathcal{C}^+(q_{k,l}+1)\tilde{\mathcal{B}}_m(\varepsilon_{k,l} - T_c)\big] \end{aligned} \tag{10}$$

with

$$\tilde{\mathcal{A}}_m(\varepsilon_{k,l}) = \frac{1}{M}\sum_{i=0}^{M-1} d_{i-Q_{k,l}-1} d_i r_m(\varepsilon_{k,l})$$

and

$$\tilde{\mathcal{B}}_m(\varepsilon_{k,l}) = \frac{1}{M}\sum_{i=0}^{M-1} d_{i-Q_{k,l}} d_i r_m(\varepsilon_{k,l}).$$

The other terms are identical to the ones introduced in Property 1.

It is worth noting that quantities $\mathcal{C}^-$ and $\mathcal{C}^+$ can interpreted as the number of pulses colliding between the two signals with delay τ_k and τ_l respectively [17]. Thus, it will be referred to as "collisions" in the sequel. We can see from Property 1 that the number of collisions between shifted signals ($\mathcal{C}^-$ and $\mathcal{C}^+$) influences the performance. However, since they are weighted by

$r_m(.)$ functions which have a time duration much smaller than the chip duration, it may happen that even if $\mathcal{C}^-(q)$ (resp. $\mathcal{C}^+(q)$) is different from 0, its contribution to $\bar{f}_m^{(k,l)}$ (resp. to $\tilde{f}_m^{(k,l)}$) can be small or even zero. Nevertheless to minimize the off-diagonal terms, it is interesting to avoid collision by minimizing the maximum of $\mathcal{C}^-$ and $\mathcal{C}^+$ as done in [18] in the context of multi-user interference.

Let $\mathcal{I}_1 = [T_g, \Delta - T_g]$, $\mathcal{I}_2 = [T_g + \Delta, T_c - T_g - \Delta]$, and $\mathcal{I}_3 = [T_c + T_g - \Delta, T_c - T_g]$ be three intervals. After simple algebraic manipulations, for PPM format, one can prove that, if $\varepsilon_{k,l} \in \mathcal{I}_1$, or if $\varepsilon_{k,l} \in \mathcal{I}_2$, or if $\varepsilon_{k,l} \in \mathcal{I}_3$, for all (k,l), then we do not encounter any overlapping. Notice that, when $\Delta < T_g$, the above condition for non-overlapping simplifies because intervals $\mathcal{I}_1$ and $\mathcal{I}_3$ become empty. For PAM format, we can ensure that both echoes τ_k et τ_l do not lead to collision if $\varepsilon_{k,l} \in \mathcal{I}_4 = [T_g, T_c - T_g]$. In such a case, the non-diagonal terms of the FIM are thus equal to zero.

In case of absence of overlapping, the terms $f_m^{(k,l)}$ are zero as soon as k is different from l and thus, the only remaining terms to calculate are $f_m^{(k,k)}$. In such a case, we have $Q_{k,k} = 0$, $q_{k,k} = 0$, and $\varepsilon_{k,k} = 0$. Then (7) and (10) lead to the same following simple equation

$$f_m^{(k,k)} = MN_f E_m \tag{11}$$

with

$$E_1 = \int g(t)g(t)dt$$
$$E_2 = \int g(t)g'(t)dt$$
$$E_3 = \int g'(t)g'(t)dt.$$

Notice that (11) holds for the PPM as well as for the PAM format. One can remark that the performance does not depend on the training sequence in the DA scheme. Consequently, we get

$$\mathrm{CRB}(A_l) = \frac{N_0}{MN_f}\frac{E_3}{2(E_1E_3 - E_2^2)} \tag{12}$$

$$\mathrm{CRB}(\tau_l) = \frac{N_0}{MN_f}\frac{E_1}{2A_l^2(E_1E_3 - E_2^2)}. \tag{13}$$

The two previous expressions were already provided in [7], [8], [9], [19], which shows, as expected, that our general CRB expression encompasses the non-overlapping case as well. Moreover, we can also interpret the non-overlapping case as the single path case ($L = 1$) since each path is not disturbed by the other paths due to the orthogonality between all the paths. Consequently, the derivations boil down to those performed for amplitude and symbol timing estimations in the context of linearly modulated signal [20], [11].

In the NDA context, the true CRB is often untractable and is often replaced with the modified CRB [11]. The modified CRB is equal to the inversion of the modified Fisher Information Matrix defined as the mathematical expectation of Eq. (5) over the data sequence $\mathbf{d}$. Consequently the derivations obtained in DA context can be easily adapted to NDA context by averaging $f^{(k,l)}$ over data sequence $\mathbf{d}$.

Notice that, in some cases, the true CRB can be derived approximately with high accuracy. At high signal to noise ration (SNR), when the so-called parameters of nuisance (herein, the symbol sequence) belong to a discrete set, it is well known that the modified CRB tends toward the true CRB [21]. Our modified CRB is thus close to the true CRB at high SNR. At low SNR, derivations for the true CRB can be achieved by the well-known approach mentioned in [20] and [4] which consists in replacing the exponential function with its second-order polynomial series expansion in (4). Finally, in [10], a closed-form expression for the true CRB is given for any SNR. Nevertheless, the derivations hold only under very restrictive conditions on the maximum delay and under the non-overlapping assumption.

IV. Simulations

In this section, we numerically evaluate the CRB in the DA context. The displayed CRB has been averaged over the time-hopping code sequence and over the training sequence assumed to be a pseudo-random white binary sequence.

For each figure, we plot the CRB which takes into account the possible paths overlapping for various model of channels and the (simplified) CRB which does not take into account the overlapping.

The design parameters of the UWB system are chosen as follows: $N_c = 4$, $N_f = 2$, $T_c = 2$ ns and $T_w = 1$ ns. The pulse shape is the second derivative of the Gaussian function [4]. We have considered a 2-PAM constellation. Unless specified, the SNR (E_b/N_0) and the number of superframe (M) are equal to 10 dB and 100 respectively.

In Fig. 1, we consider an academic context: two paths with amplitudes $A_1 = 1$ and $A_2 = 0.5$, and with delays $\tau_1 = 0$ and $\tau_2 = \delta\tau$. We focus on the estimation of the first path τ_1.

More precisely, we plot the CRB without taking into account the echoes overlap, the CRB with taking into account the possible overlap between echoes, and the normalized mean square error (MSE) of the estimate introduced in [4]. This estimate corresponds to the ML in the absence of overlapping. The normalized MSE stands for the MSE divided by T_g^2.

We observe that the difference between both CRBs occurs when the time difference between two echoes is less than half the pulse duration. We also remark the ML-like estimate is far way from the optimal performance in case of strong overlap.

We now want to know if the situation for which the overlapping can not be neglected (*i.e.*, for which there exists small time difference between two paths) appears sufficiently often in a realistic model of channel for disturbing notably the estimation performance. Therefore, in the rest of this section, we consider the standard model used in IEEE test environment and introduced by Molish in [14], [15]. For the sake of simplicity, we consider only one cluster, then we recall that the difference between two consecutive delays satisfies an exponential distribution with parameter λ. The parameter λ obviously represents the path density since the mean time difference between two echoes is actually equal to $1/\lambda$. Finally, the amplitudes are obtained as $A_l = a_l e^{-\tau_l/\gamma}$ where a_l can be decomposed as the following product $a_l = p_l b_l$ with $p_l \in \{-1, +1\}$ an equally distributed binary process and b_l a log-normal process. One can notice that the parameter γ is the root mean square delay spread. Moreover, the paths obey the following normalization condition $\sum_{l=1}^{L} \gamma_l^2 = 1$. For the Molish's channel model, we consider two sets of parameters: on one hand, the set $\gamma = 4.3$ns and $\lambda = 2.5$ns^{-1} ($1/\lambda = 0.4$ns) associated with the so-called CM1 channel, and on the other hand, the set $\gamma = 6.7$ns and $\lambda = 0.5$ns^{-1} ($1/\lambda = 2$ns) associated with the so-called CM2 model and also introduced in [22]. On Fig. 1, we observe that if the time difference between two paths is smaller than 0.1 ns, then the estimation error is of order of that time difference and any estimation procedure wil be able to distinguish one path from another one. Therefore we have discarded too close adjacent paths (smaller than 0.1 ns) as well as the paths associated with too small magnitude (smaller than 10^{-2}). The curves are averaged over 1000 Monte-Carlo trials for which the paths are modified at each run.

In order to handle all the paths, we sum the Cramer-Rao bound in the following way $\text{CRB}(\boldsymbol{\tau}) = \frac{1}{L}\sum_{l=1}^{L} \text{CRB}(\tau_l)$. Notice that we focus on delay estimation rather than on amplitude estimation because it is a more crucial issue for system performance. Obviously, the CRB on delay parameter takes into account the amplitude estimation step.

In Fig. 2 and Fig. 3, the MSE are plotted versus E_b/N_0 and λ respectively. We notice that the performance for CM2 model is almost insensitive to overlapping. In contrast, there is a gap for the CM1 model. Actually, according to the value of λ, CM1 model leads to several close paths since the main time difference between two echoes is less than half a pulse duration whereas the time difference between two consecutive paths is much larger for the CM2 model. As a conclusion, we can see that the overlapping degrades dramatically the performance if the time difference is much less than T_g, which may occur in realistic situations.

V. Conclusion

In this paper, we have derived in closed-form expression the CRB for the delay and the attenuation of each path of the UWB propagation channel. Unlike existing literature, the derivations had taken into account the possible overlap between different paths. In the simulation part, we have observed that the estimation performance obtained in standard channel model needed the assumption of overlap between echoes to be valid.

Appendix

After algebraic manipulations relying on (1), we obtain:

$$\begin{aligned} f_m^{(k,l)} &= \sum_{i_1,i_2=0}^{M-1} \sum_{j_1,j_2=0}^{N_f N_c-1} c(j_1)c(j_2) \\ &\times \quad r_m(\delta i N_f T_f + \delta j T_c + \Delta(d_{i_1} - d_{i_2}) + \tau_k - \tau_l) \end{aligned}$$

with $\delta i = i_1 - i_2$, $\delta j = j_1 - j_2$ and

$$\begin{aligned} r_1(\tau) &= \int g(t-\tau)g(t)dt \\ r_2(\tau) &= \int g(t-\tau)g'(t)dt \\ r_3(\tau) &= \int g'(t-\tau)g'(t)dt. \end{aligned}$$

By using (6), we get

$$\begin{aligned} f_m^{(k,l)} = \sum_{i_1,i_2=0}^{M-1} \sum_{j_1,j_2=0}^{N_f N_c-1} c(j_1)c(j_2) r_m((\delta i + Q_{k,l}) N_f T_f \\ + (\delta j + q_{k,l})T_c + \Delta(d_{i_1} - d_{i_2}) + \varepsilon_{k,l}). \end{aligned} \tag{14}$$

Inasmuch as the support of $\tau \mapsto r_m(\tau)$ is $(-T_g, T_g)$, a lot of terms in (14) are zero since the term $r_m((\delta i + Q_{k,l})N_f T_f + (\delta j + q_{k,l})T_c + \Delta(d_{i_1} - d_{i_2}) + \varepsilon_{k,l})$ is different from 0 if and only if

$$-T_g < (\delta i + Q_{k,l})N_f T_f + (\delta j + q_{k,l})T_c + \Delta(d_{i_1} - d_{i_2}) + \varepsilon_{k,l} < T_g. \tag{15}$$

We recall that

$$-\Delta \leq \Delta(d_{i_1} - d_{i_2}) \leq \Delta$$

$$-N_c N_f + 1 \leq \delta j + q_{k,l} \leq 2N_c N_f - 1$$

and

$$0 < \varepsilon_{k,l} < T_c.$$

Consequently, by replacing $\Delta(d_{i_1} - d_{i_2})$, $\delta j + q_{k,l}$ and $\varepsilon_{k,l}$ with their upper and lower bounds in (15), we obtain that

$$-T_g - \Delta - 2N_f T_f + T_c < (\delta i + Q_{k,l})N_f T_f \leq N_f T_f - T_c + \Delta + T_g$$

i.e.,

$$-2 + \frac{T_c - \Delta - T_g}{N_f T_f} < \delta i + Q_{k,l} \leq 1 - \frac{T_c - \Delta - T_g}{N_f T_f}.$$

As the PPM shift Δ is smaller than $T_c - T_g$, we get the following constraint on the summation indices i_1 and i_2:

$$-2 < \delta i + Q_{k,l} < 1$$

which implies that

$$i_1 - i_2 = -Q_{k,l} - 1 \qquad \text{or} \qquad i_1 - i_2 = -Q_{k,l}.$$

Therefore, expression (14) can be decomposed as follows:

$$f_m^{(k,l)} = \bar{f}_m^{(k,l)} + \tilde{f}_m^{(k,l)}$$

with

$$\begin{aligned} \bar{f}_m^{(k,l)} \quad = \quad & \sum_{i_2=0}^{M-1} \sum_{j_1,j_2=0}^{N_c N_f - 1} c(j_1)c(j_2) r_m\big(- N_f T_f \\ & + (\delta j + q_{k,l})T_c + \Delta(d_{i_2 - Q_{k,l} - 1} - d_{i_2}) + \varepsilon_{k,l}\big) \end{aligned}$$

which corresponds to the summation over i_1 and i_2 with the constraint $i_1 - i_2 = -Q_{k,l} - 1$ and with

$$\begin{aligned}\tilde{f}_m^{(k,l)} &= \sum_{i_2=0}^{M-1} \sum_{j_1,j_2=0}^{N_cN_f-1} c(j_1)c(j_2)r_m\big((\delta j + q_{k,l})T_c \\ &\quad +\Delta(d_{i_2-Q_{k,l}} - d_{i_2}) + \varepsilon_{k,l}\big)\end{aligned}$$

which corresponds to the summation over i_1 et i_2 with the constraint $i_1 - i_2 = -Q_{k,l}$.

Let us consider first the calculation of $\bar{f}_m^{(k,\ell)}$. As $i_1 - i_2 = -Q_{k,l} - 1$, the constraint (15) can be simplified in the following way

$$-T_g \leq (\delta j + q_{k,l} - N_cN_f)T_c + \Delta(d_{i_2-Q_{k,l}-1} - d_{i_2}) + \varepsilon_{k,l} \leq T_g.$$

Since T_g is assumed smaller than T_c and Δ smaller than $T_c - T_g$, we get

$$-2 < \delta j + q_{k,l} - N_cN_f < 1$$

which implies that

$$\bar{f}_m^{(k,l)} = g_m^{(k,l)} + h_m^{(k,l)}$$

where $g_m^{(k,l)}$ is the term associated with the summation over j_1 and j_2, satisfying the constraint $j_1 - j_2 + q_{k,l} - N_cN_f = 0$ and where $h_m^{(k,\ell)}$ is the term associated with the summation over j_1 and j_2, satisfying the constraint $j_1 - j_2 + q_{k,l} - N_cN_f = -1$.

Thus, we have

$$\begin{aligned}g_m^{(k,l)} &= \sum_{i=0}^{M-1} \sum_{j_1=N_cN_f-q_{k,l}}^{N_cN_f-1} c(j_1)c(j_1 + q_{k,l} - N_cN_f) \\ &\quad r_m\big(\Delta(d_{i-Q_{k,l}-1} - d_i) + \varepsilon_{k,l}\big).\end{aligned}$$

By setting $j = j_1 + q_{k,l} - N_cN_f$, we obtain

$$\begin{aligned}g_m^{(k,l)} &= \sum_{i=0}^{M-1} \sum_{j=0}^{q_{k,l}-1} c(j + N_cN_f - q_{k,l})c(j) \\ &\quad r_m\big(\Delta(d_{i-Q_{k,l}-1} - d_i) + \varepsilon_{k,l}\big).\end{aligned}$$

Thanks to the codes' periodicity, we can write the following result

$$g_m^{(k,l)} = \sum_{i=0}^{M-1} \mathcal{C}^-(q_{k,l})r_m\big(\Delta(d_{i-Q_{k,l}-1} - d_i) + \varepsilon_{k,l}\big) \tag{16}$$

In the same way, we can show that

$$\begin{aligned} h_m^{(k,l)} &= \sum_{i=0}^{M-1} \mathcal{C}^-(q_{k,l}+1) \\ &\quad r_m\big(\Delta(d_{i-Q_{k,l}-1} - d_i) - T_c + \varepsilon_{k,l}\big). \end{aligned} \tag{17}$$

The calculation of the $\tilde{f}_m^{(k,l)}$ can be achieved similarly and leads to the following expression

$$\begin{aligned} \tilde{f}_m^{(k,l)} &= \sum_{i=0}^{M-1} \mathcal{C}^+(q_{k,l}) r_m(\Delta(d_{i-Q_{k,l}} - d_i) + \varepsilon_{k,l}) \\ &+ \sum_{i=0}^{M-1} \mathcal{C}^+(q_{k,l}+1) \\ &\quad r_m(\Delta(d_{i-Q_{k,l}} - d_i) - T_c + \varepsilon_{k,l}) \end{aligned} \tag{18}$$

By merging (16), (17), and (18), we conclude the proof.

REFERENCES

[1] F. Ramirez-Mireles and R. A. Scholtz, “Multiple access performance limits with time-hopping and pulse-position modulation,” *International Conference on Acoutics, Speech, and Signal Processing (ICASSP)*, 1998, pp. 529-533.

[2] M. Z. Win and R. A. Scholtz, “Ultra-Wide Bandwidth time-hopping spread-spectrum impulse radio for wireless multiple access communications,” *IEEE Trans. on Communications*, vol. 48, no. 4, pp. 679-691, Apr. 2000.

[3] M. Z. Win and R. A. Scholtz, “On the energy capture of Ultrawide bandwidth signals on dense multipath environments,” *IEEE Communications Letters*, vol. 2, no. 9, pp. 245-247, Sep. 1998.

[4] V. Lottici, A. N. D’Andrea and U. Mengali, “Channel estimation for Ultra-Wideband communications,” *IEEE Journal on Selected Areas in Communications*, vol. 20, no. 9, pp. 1638-1645, Dec. 2002.

[5] I. Maravic and M. Vetterli, “Low-Complexity subspace methods for channel estimation and synchronization in Ultra-Wide band systems,” *International Workshop on Ultra-Wide Band (IWUWB)*, May 2003.

[6] X. Luo, and G. B. Giannakis, "Blind timing and channel estimation for UWB multi-user ad hoc access", *in Proc. of Asilomar Conference*, Nov. 2004.

[7] N. Laurenti, T. Erseghe, and T. Cellini, "On the performance of TH-PPM and TH-PAM as transmission formats for UWB communications", *in Proc. of the IEEE Vehicular Technology Conference*, Sept. 2004.

[8] L. Huang and C. Chung Ko, "Performance of maximum likelihood channel estimator for UWB communications, *IEEE Communications Letters*, Jun. 2004.

[9] J. Zhang, R. Kennedy, and T. Abhayapala, "Cramer-Rao lowerbounds for the time delay estimation of UWB signals", *in Proc. of ICC*, Jun. 2004.

[10] Y. Chen, and N. C. Beaulieu, "CRLBs for NDA ML estimation of UWB channels", *IEEE Communications Letters*, pp. 709- 711, Aug. 2005.

[11] A. N. D’Andrea, U. Mengali and R. Reggiannini, “The modified Cramer-Rao bound and its application to synchronisation problem,” *IEEE Trans. on Communications*, vol. 42, no. 2/3/4, pp. 1391-1399, Feb. 1994.

[12] G. Durisi, and G. Romano, “On the validity of Gaussian approximation to characterize the multiuser capacity of UWB TH-PPM,” in *Proc. IEEE Conference on Ultra Wideband Systems and Technologies 2002, Digest of Papers*, Baltimore, USA, pp. 157-162.

[13] J. Fiorina, and W. Hachem, "Central Limit Results for the Multiple User Interference at the SUMF Output for UWB Signals", in *ISITA*, Parma, Italy, 2004.

[14] A. F. Molish, J. R. Foerster, and M. Pendergrass, "Channel models for ultrawideband personal area networks", *IEEE Wireless Communications*, vol. 10, pp. 14-21, Dec. 2003.

[15] A. F. Molish, K. Balakarishanan, and D. Cassioli, "IEEE 802.15.4a channel model - final report", Technical Report (IEEE 802.15-04-0662-02-004a), 2005.

[16] C. J. Le Martret and G. B. Giannakis, “All-digital impulse radio for wireless cellular systems,” *IEEE Transactions on Communications*, vol. 50, no. 9, pp. 1440-1450, Sep. 2002.

[17] C. J. Le Martret, A.-L. Deleuze, and P. Ciblat, "Optimal Time-Hopping Codes for Multi-User Interference Mitigation in Ultra-Wide Bandwidth Impulse Radio," *IEEE Trans. on Wireless Communications*, Vol. 5, No. 6, June 2006.

[18] M. B. Pursley, "Performance evaluation for coded spread-spectrum multiple access communication", *IEEE Trans. on Communications*, vol. 25, pp. 795-799, Aug. 1977.

[19] A.-L. Deleuze, C. J. Le Martret, and P. Ciblat, "Cramer-Rao bound for channel parameters in Ultra-Wide Band based system", *IEEE Workshop on Signal Processing Advances in Wireless Communications (SPAWC)*, Lisbon (Portugal), Jul. 2004.

[20] S. M. Kay, *Fundamentals of Statistical Signal Processing: estimation theory*, Englewood Cliffs, Prentice-Hall, 1993.

[21] M. Moeneclaey, "In the true and the modified Cramer-Rao bounds for the estimation of a scalar parameter in the presence of nuisance parameters", *IEEE Trans. on Communications*, vol. 46, pp. 1536-1544, Nov. 1998.

[22] H. Lee, B. Han, Y. Shin and S. Im, “Multipath characteristics of impulse radio channels,” *IEEE Vehicular Technology Conference (VTC)*, pp. 2487-2491, 2000.

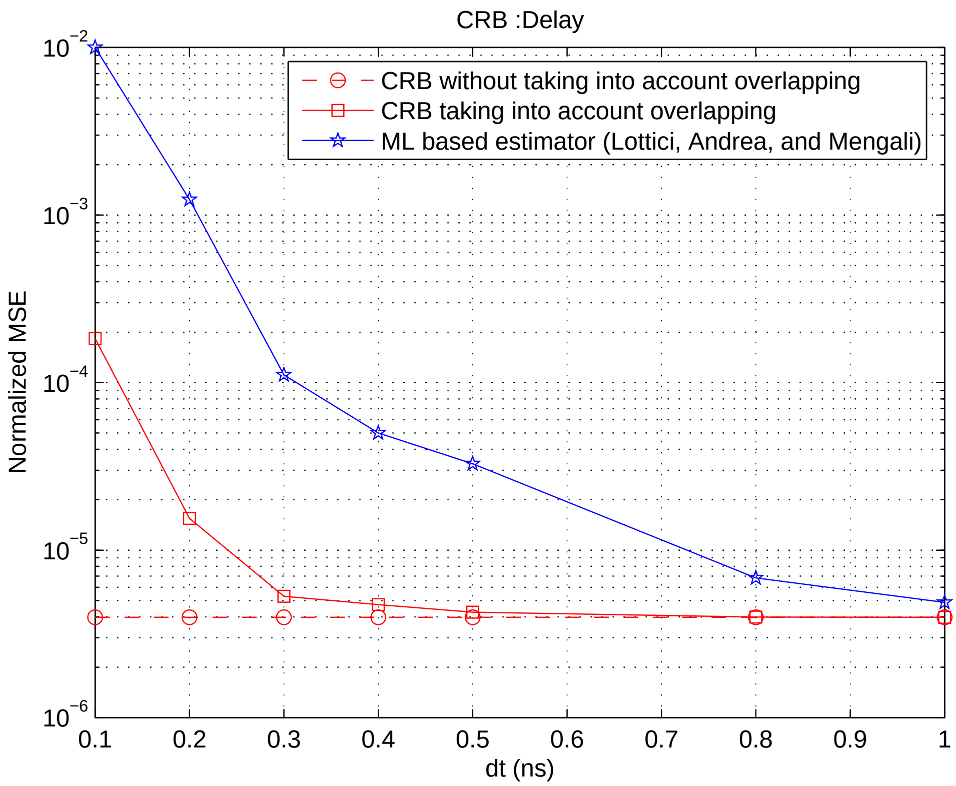

Fig. 1. $\mathrm{CRB}(\tau)_{|\tau=0}$ versus $\delta\tau$

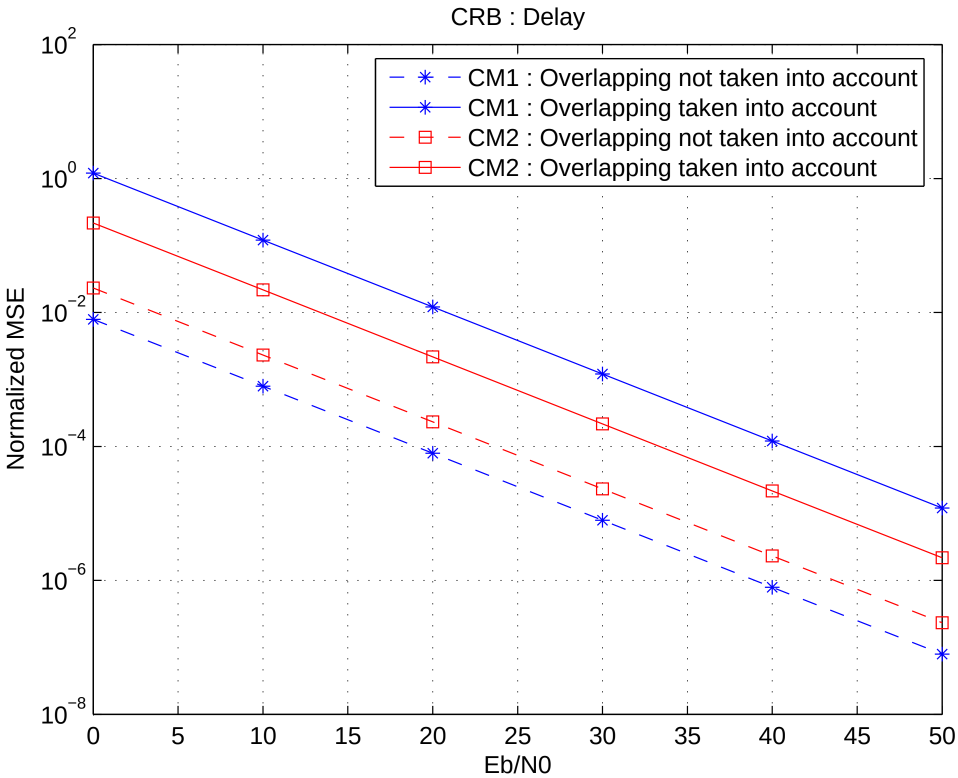

Fig. 2. CRB($\boldsymbol{\tau}$) versus E_b/N_0

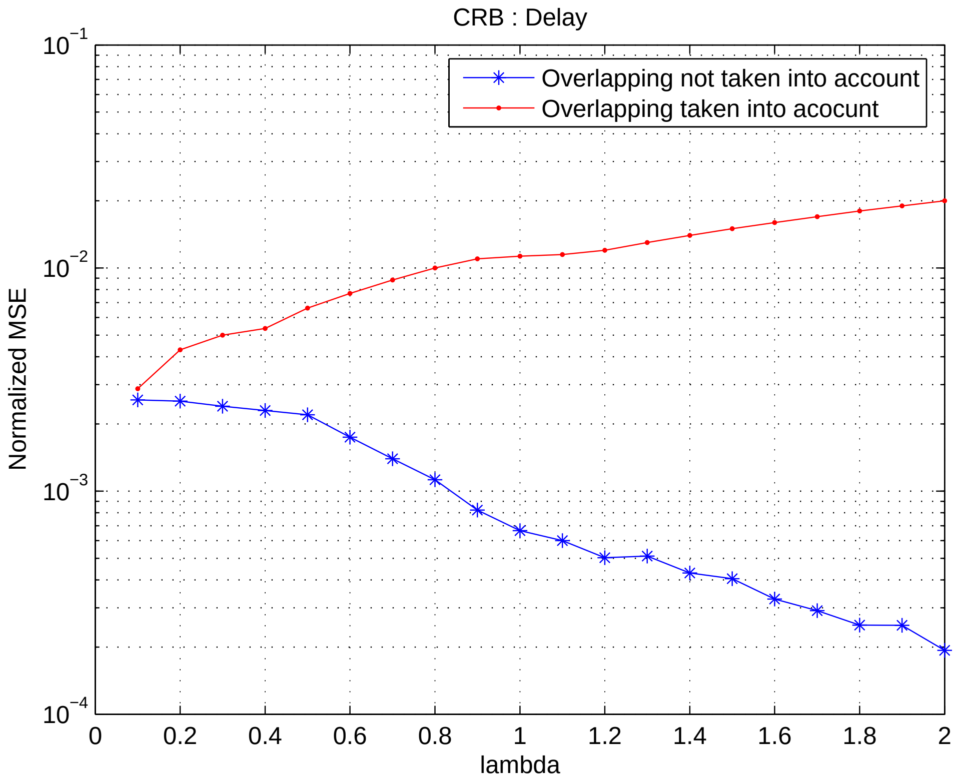

Fig. 3. CRB(τ) versus λ